JOURNAL OF MATERIALS SCIENCE 27 (1992) 2946–2951

Vaporization rates from sintered bodies and single crystals of NaCl in flowing air

T. SATA
Department of Industrial Chemistry, Kumamoto Institute of Technology, Ikeda, Kumamoto 860, Japan

Weight losses by vaporization from NaCl sintered bodies and single crystals ((1 0 0) and (1 1 1) surfaces) were measured in flowing dry air at temperatures from 500–700 °C for up to 1150 h. Plots of log weight losses against log time at the respective temperatures gave straight lines. At temperatures less than 600 °C, induction periods of up to 10^5–10^6 s were seen, during which the vaporization rates were abnormally smaller. After these periods finished, vaporization took place at constant rates, and activation energies indicated similar values to the heat of vaporization. The vaporization rates were higher for the sintered bodies than those for the single crystals. During vaporization, microstructures appeared on the vaporized surfaces transferred through roof structure (1 1 0) to pyramid structure (1 1 1) for all the specimens.

1. Introduction

The NaCl body is useful as a basic model for ionic oxide ceramics and its easy treatment in experiments makes it suitable for use as a model in materials science and technology. NaCl bodies are used as materials for optical devices or solvents for growing single crystals. Several industrial problems relating to the chemical reactions with the NaCl vapours are encountered: the NaCl vaporizes in the burning of waste in cities, and subsequently corrodes the refractories lining the furnace; NaCl mist in coastal regions deteriorates metallic materials and electronic circuits; NaCl vapour reacts with earthernware in the firing kiln to produce a salt glaze on the pipes used for waste water. Thus NaCl vapour contained in small concentrations in the air around us has important implications in the fabrication and properties of pure ceramics.

Many papers on the equilibrium vaporization of NaCl have been published and thermodynamic data for solid, liquid and gaseous species were obtained from these results [1]. Vapour pressures have been measured by several methods [2]: the boiling point method, Rodenbush–Dixon technique, the transpiration and effusion methods, and mass spectrometry for vapour effused from a cell. Results on the mass spectrometric vapour pressure measurements on the systems NaCl–KCl and NaCl–MnCl have been published [3–5].

In the present study, changes in the vaporization rate with temperatures and flow rates of air were measured using the transpiration method and changes in the structure during vaporization were observed in the temperature range 500–700 °C. A transpiration study of NaCl was performed by Hlavac *et al.* [6] and the vapour pressures obtained were consistent with the data published in the literature [1]. Leister and Somorjai [7] discussed the vapour pressure values in relation to the dislocation densities, and showed lower pressures from the surface (1 0 0) of a single crystal NaCl having 10^6 dislocations/cm^2 compared to the equilibrium one of 10^7 dislocations/cm^2. Bethge and colleagues [8, 9] also mentioned the propagation of a monoatomic straight step. Knoppik and Penningsfeld [10] observed the changes in surface morphologies of (1 0 0), (1 1 0) and (1 1 1) during vaporization up to 800 °C and 9 h in vacuum. Munir [11] reported sequential changes of the step features on the (1 0 0) surface of single crystals during short-term vaporization in the temperature range from 320–520 °C, related to the presence of several types of dislocation. There has been no study previously reported of the vaporization in an air flow and structural changes over a longer term, up to about 1150 h (max).

2. Experimental procedure

2.1. Fabrication of sintered bodies

A saturated NaCl (99.9% purity; metallic impurities 0.0005% Pb, 0.0003% Fe, 0.001% Ca, 0.001% Ba, 0.005% K) solution (26%) was cooled to − 20 °C, and acetone, at the same temperature, was added to this solution thus preventing any significant temperature rise. The precipitated NaCl was rapidly filtered and washed twice with acetone, and then was immediately heated to 400 °C and completely dried at 400 °C overnight. No crystal growth was seen at this temperature. The dried powders were preserved in a desiccater. The powder was cubic in shape and had a homogeneous cubic size of 1.8 μm, as observed by scanning electron microscopy (SEM). The powders were compacted under a pressure of 1 t cm^{-2} to pellets of 13 mm diameter and sintered in air at 650 °C for 3 h. Their

0022–2461

relative densities were 93%–95%. This powder fabrication and sintering has been described [12].

2.2. Fabrication of single crystals

The pure NaCl was fused in a mullite crucible above the melting point (801 °C) and pulled up at rates of 10–20 mm h^{-1}, and also at rotations of 20–25 r.p.m. (Czochralski method). The (1 0 0) face was generally obtained even without a seed. The (1 1 1) face was grown when using a seed. The as-grown single crystal was shaved to about 10 mm diameter using a lathe and then cut to 0.2–1 mm thickness.

2.3. Vaporization

Specimens, 10–13 mm diameter, 0.2–1 mm thick, were used for the vaporization after polishing of the surfaces with an abrasive paper of fine SiC (no.1200) and then by cloth with a little water. Then, the specimen was rapidly dried by heating. The air dried using silica gels was used as a carrier gas for the vapour and its flow rate was kept constant at 200 ml min^{-1} through a mullite pipe of 20 mm diameter. The linear flow rate corresponds to about 1 cm s^{-1} at room temperature.

This specimen on a platinum plate was placed in a mullite boat and inserted into a homogeneous temperature region of a mullite tube (20 mm diameter) heated using SiC heaters. At first, the specimen was inserted at a temperature 200 °C below the running temperature, and the weight of the specimen was confirmed to be constant; then the temperature was raised rapidly by insertion of the boat into the running temperature region. The weights were determined after cooling every 3 h in the first day. The weight losses of the specimen due to the vaporization were determined up to the microgram level using a microbalance (Sartorius, μg sensitivity, 30 g max). Such a determination was repeated after each vaporization. Vaporization loss was calculated as the weight loss per unit surface area (g cm^{-2}) of the pellet-type specimen. Temperatures were determined with a Pt–13%Rh thermocouple, which was located at the nearest side of the specimen, and were controlled to within ± 7 °C.

3. Results and discussion

3.1. Effect of flow rate of air

In Fig. 1 the vaporization rates, V (g cm^{-2} s^{-1}), obtained from experiments over 2–4 h are shown plotted against various linear flow rates, F (cm s^{-1}), of the dried air as straight lines, and are represented by

$$V = a + bF \quad (1)$$

The approximate values of a and b and activation energy, E, were calculated from the equation at three temperature levels only. The respective values of activation energy, 227 and 209 kJ mol^{-1}, nearly correspond to the heat of vaporization of 229 kJ mol^{-1} [1]. From the above flow-rate effects, a constant rate of 200 ml min^{-1} was adopted in this study to determine the weight loss values and to increase the accuracy of the microbalance.

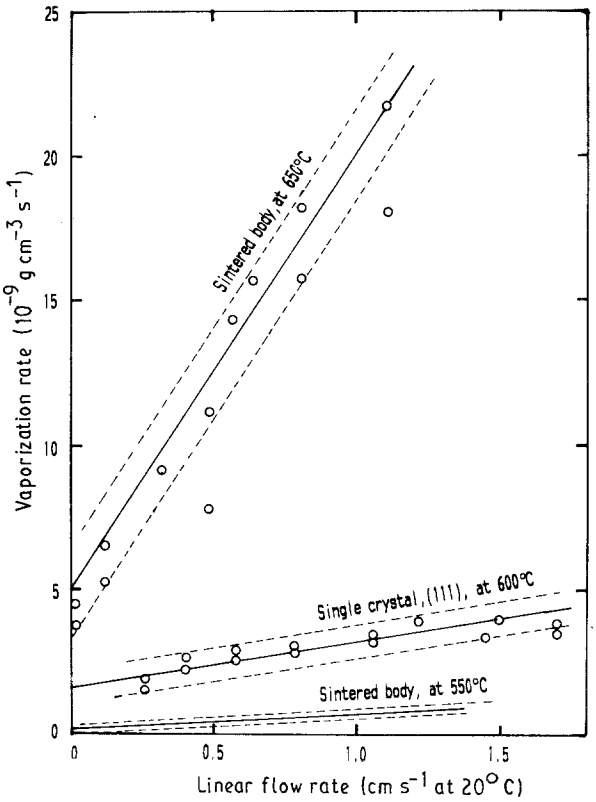

Figure 1 Linear relations of vaporization rates for sintered bodies and single crystals of NaCl plotted against linear flow rates of air.

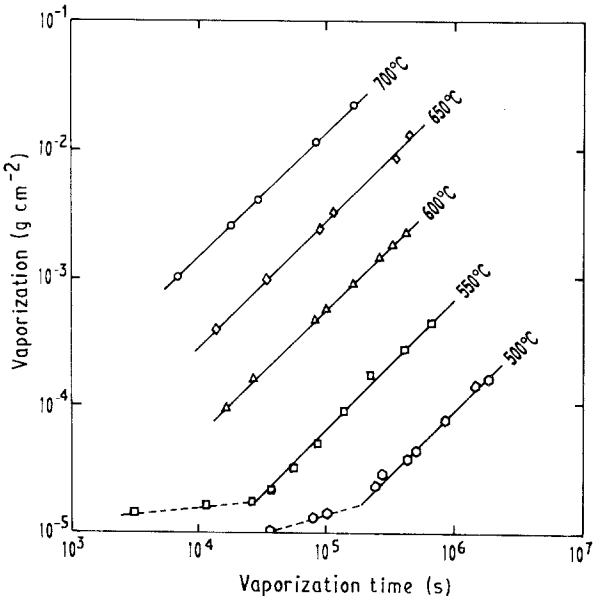

Figure 2 Vaporization from sintered NaCl in flowing air plotted against vaporization time.

3.2. Vaporization results

Fig. 2 shows the relationship of vaporization (g cm^{-2}) versus vaporization time(s) for the sintered specimens. It is noted that induction periods up to 4–140 h are seen in early stages at temperatures lower than 600 °C, and elongate with lowering temperatures. Lower

TABLE I Results of vaporization from NaCl bodies

	Temperature (°C)	Total vaporization time (h)	Vaporization %	Transition of slope (h)	Slope in early stage	Vaporization rate (10^{11} g cm^{-2} s^{-1})	Slope in later stage
Sintered bodies	700	75	22.92	–	–	13900	0.972
	650	155	6.57	–	–	2690	0.997
	600	118	1.519	4	–	519	0.984
	550	353	0.234	8	0.11	66.6	1.028
	500	527	0.105	54	0.31	8.97	0.997
						(mean	0.996)
Single (1 0 0) crystals	700	76	12.10	–	–	5500	0.939
	650	189	4.29	–	–	2275	0.946
	600	502	3.58	4	–	310	1.032
	550	184	0.455	16	0.73	54	1.064
		–	–	–	–	65	1.073
		358	0.41	–	–	68	1.139
	500	1148	0.28	139	0.75	8.8	0.963
						(mean	1.004)
(1 1 1)	600	155	2.09	10	–	404	1.136
	550	178	0.557	18	0.17	72.3	1.065

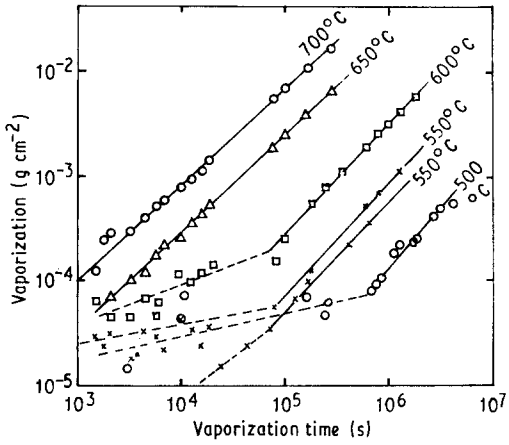

Figure 3 Vaporization from (1 0 0) surfaces of NaCl single crystals in flowing air plotted against vaporization time.

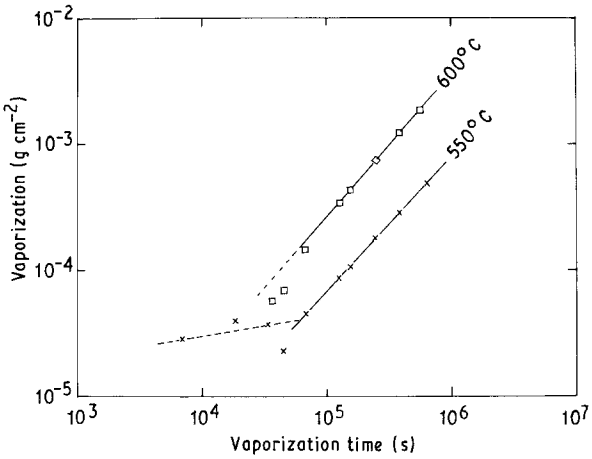

Figure 4 Vaporization from (1 1 1) surfaces of NaCl single crystals in flowing air plotted against vaporization time.

values (< 1) for slopes are also seen; the slopes are listed in Table I with other results.

Fig. 3 shows results for the (1 0 0) surface of the single crystal. Here, too, the same induction periods with smaller slopes are seen, especially at temperatures of 500–600 °C. These data are also listed in Table I. The results for the (1 1 1) surface of the single crystal are presented in Fig. 4, which also shows the induction periods. After the above induction periods, constant rates of vaporization (slope = 1) continue. Logarithm of the constant vaporization rates was plotted against $1/T$, and the activation energies were calculated to be 218 kJ mol^{-1} for the sintered body, 214 kJ mol^{-1} for the (1 1 0) surface of the single crystal, and 201 kJ mol^{-1} for the (1 0 0) surface. The smallest value for the (1 0 0) surface indicates the congruent vaporization of both sodium and chlorine as NaCl molecules from ledge sites. These values are slightly smaller compared to the heat of vaporization of 208–231 kJ mol^{-1} for the second law (229 kJ mol^{-1} as the third law value [1]).

3.3. Microstructures of the surfaces after vaporization

Representative scanning electron micrographs for the specimens after vaporization are shown in Fig. 5 for the sintered bodies and in Fig. 6 for the single crystals representing typical structures named A–G. In Fig. 5, the A structure mostly corresponds to the original one, but shoulders of grain boundaries become rounded from the polished surface. In particular, the vaporization seemed to start only from traces of mechanical scratches, impurity spots and triple points of the grain boundary. Structure B has large pores produced by coupling of these points. Structure D has rectangular grains and pores and the grain-boundary grooves become deeper and wider. Type C structure (not shown) is a mixture of B and D. Structure E shows long roofs which seem to be (1 1 0) morphology with many (1 0 0) steps which then change to short roofs. Fig. 7a shows the transfer (A–B–C–D–E) of microstructure on the vaporized surface of the sintered body with vaporization times.

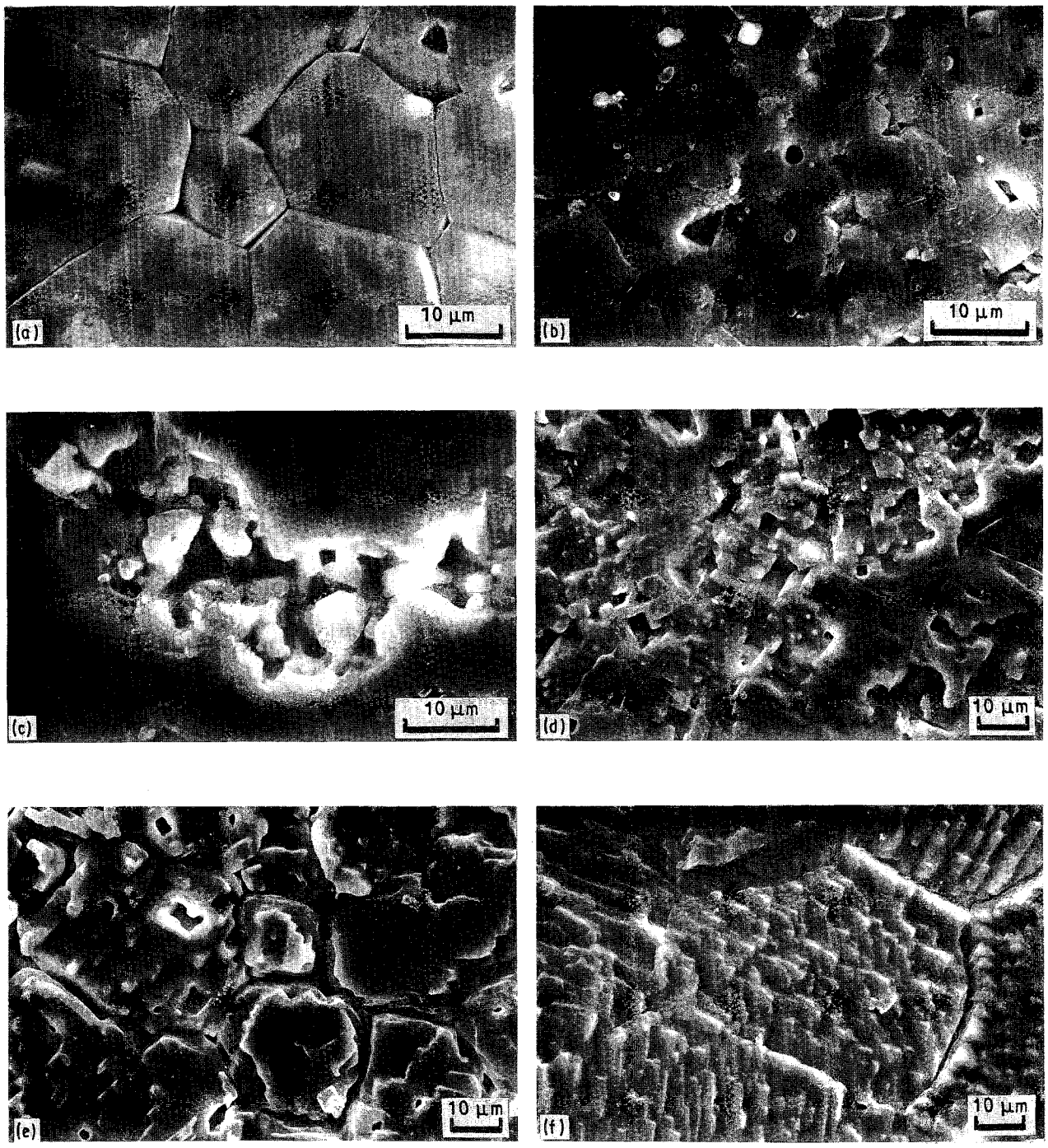

Figure 5 Scanning electron micrographs after vaporization from sintered NaCl, showing the surface morphologies A, B, D and E. (a) Type A, 600 °C, 122 min; (b) Type A, 600 °C, 360 min; (c) Type B, 600 °C, 1200 min; (d) Type D, 550 °C, 353 h; (e) Type D, 600 °C, 118 h; (f) Type E, 650 °C, 155 h.

Changes on the single-crystal surface (1 0 0) as shown in Fig. 6, are very similar to those of the sintered body. Type A structure is the original polished surface without grain boundaries. Structure D begins to appear as rectangular grains rising up on the surface and then this structure changes to Type E structure with the long roofs. These roofs shorten and transform to G structure, which has triangular or hexagonal faces and seems to show (1 1 1)-like morphology. At 700 °C whiskers were formed at grain boundaries and were also deposited inside the wall of the tube. Such structure transformations are indicated in Fig. 7b, where the same order of A–D–E–G as that for single grain of the sintered body is seen.

Surface structure changes during the vaporization of NaCl single crystals in shorter times and a vacuum have already been described. Knoppik and Penningsfeld [7] reported step formations on (1 0 0), (1 1 1) and (1 1 0) surfaces after 1 and 9 h in vacuum. The (1 0 0) surface showed a terrace formation up to 800 °C, the (1 1 1) surface a triangular shape at 650 °C, and the (1 1 0) surface long roofs at 600 °C for 1 h. These results for shorter times are consistent with those in this study. In spite of such a characteristic change in the surface structure, the above apparent orientation was not detected on the X-ray diffraction (XRD) patterns, even after several hundred hours. Thus, it is considered that the apparent roofs and triangular tops (pyramids) are oriented with respect to the original face with many steps and terraces. As a

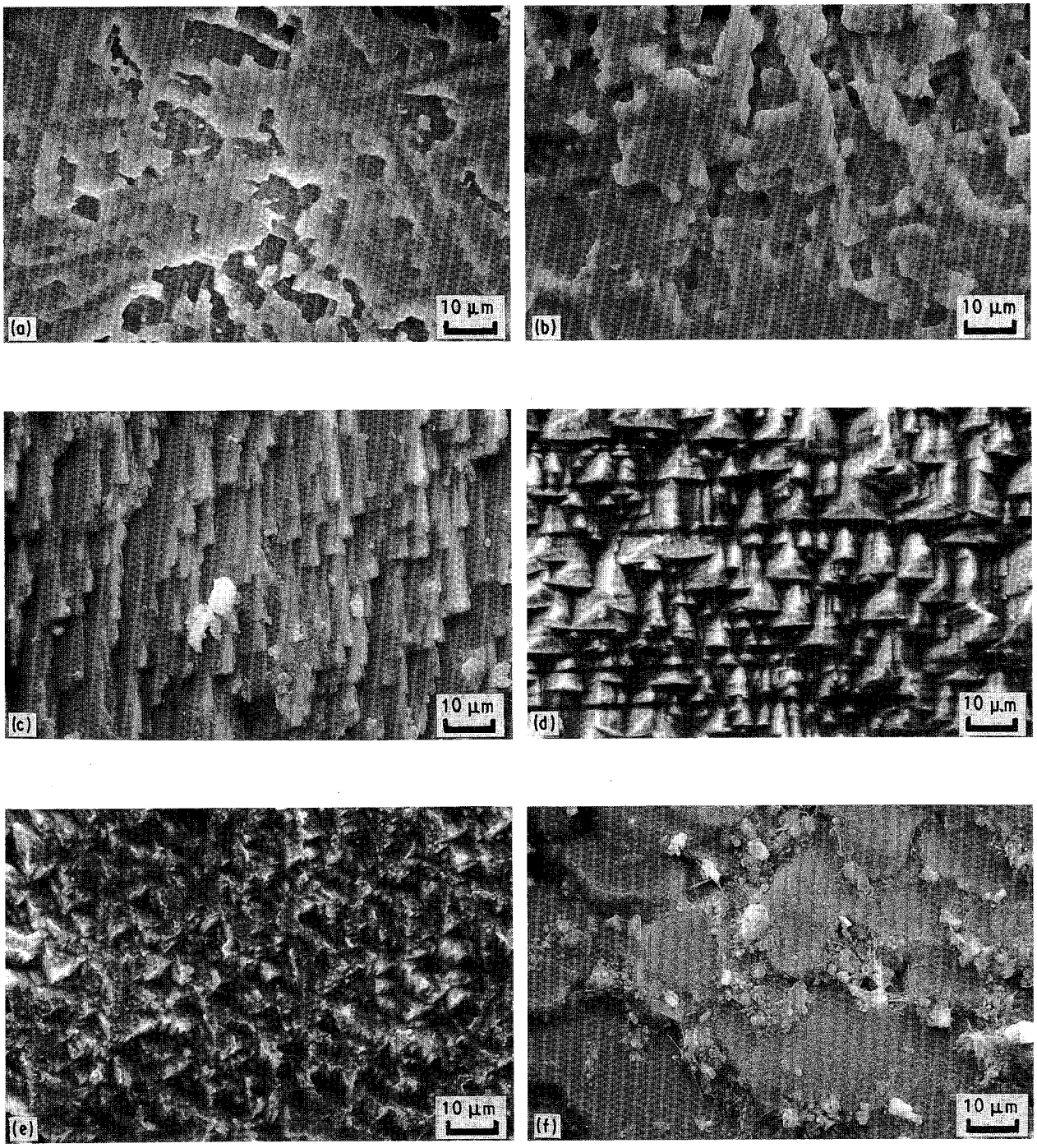

Figure 6 Scanning electron micrographs after vaporization from (1 0 0) and (1 1 1) surfaces of single crystals of NaCl showing the surface morphologies D, E and G. (a) Type D, (1 0 0), 550 °C, 184 h; (b) Type D, (1 0 0), 550 °C, 358 h; (c) Type E, (1 0 0), 600 °C, 502 h; (d) Type E, (1 1 1), 600 °C, 155 h; (e) Type G, (1 1 1), 550 °C, 178 h; (f) Type G, (1 0 0), 700 °C, 76 h.

final result it is shown that all the surfaces of NaCl transform to the most stable face (1 1 1) at high temperatures.

3.4. Early stage of vaporization

Figs 2–4 show the presence of induction periods having slopes of less than 1, as indicated in Table I. These slope values were 0.1–0.7. Thus the vaporization rate decreased with vaporization time during this induction period. The transition time from the induction period (slope < 1) to the normal period (slope $= 1$) increased with decreasing temperatures, as shown by the dotted line in Fig. 7. It was found that these transitions occurred during the period when Type A structure was present at temperatures less than 600 °C. This 600 °C (873 K) corresponds to about 0.8 of the melting point ($T_m = 1074$ K) of NaCl. Above 600 °C, ions consisting of the lattice of NaCl begin to move or diffuse to construct new stable faces which have many kinks and ledges from the smooth plane initially polished. 500 °C corresponds to 0.71 T/T_m. So the values of 0.7–0.8 (at 500–600 °C) correspond to the so-called Tamman temperature. Knoppik and Penningsfeld [10] observed the beginning of changes in morphology and coarsening above 600 °C. Heyrand and Metois [13] observed the start of blunting of the summit in a single-crystal particle above 650 °C.

The perfect desorption of absorbed gas should also be considered. Knoppik and Penningsfeld [10] showed

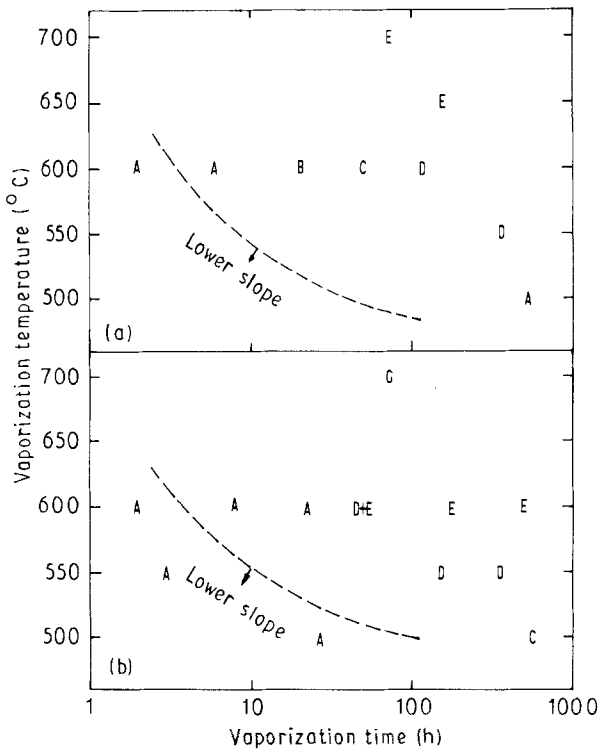

Figure 7 The variation of morphology (A–G) after vaporization from (a) the sintered bodies and (b) single crystals (1 0 0) of NaCl with vaporization temperature and time.

this desorption temperature at 450 °C for 1 h and 600 °C for 0 h in vacuum, thus this region corresponds to the presence of absorbed gas at the step sites in this study. The vaporization in this period takes place only at special points of structure defects, dislocation exits, cracks, summits of the grains, or thermal etch pits which are partially located in grains or grain boundaries. It is understood that, after the overall formation of a structure with many ledges or kinks suitable to take the constant vaporization to completion, normal vaporization is able to continue. Fig. 7 shows that these transition times for the single crystals are longer than those for the sintered body. This fact is considered reasonable.

3.5. Vaporization rates from the sintered body and single crystal

Table II shows ratios of the vaporization rates compared to those from (1 0 0) surfaces of the single crystal. The vaporization rates from the sintered body and the (1 1 1) surface of the single crystal are higher than those from the (1 0 0) surface of the single crystal. Therefore, the vaporization rate depends on the numbers of vaporization sites. The polycrystalline structure has many ledges or kinks and various defects, and the (1 0 0) surface of the single crystal has a smaller number of these, in spite of the change in surface structure during vaporization. The higher vaporization rates from the (1 1 1) surface than the (1 0 0) surface are supposed to be related to the faster formation of triangular pyramids on the (1 1 1) surface.

TABLE II Vaporization rates compared to those from the (1 0 0) surface

Temperature (°C)	Sintered body	(1 0 0)	(1 1 1)
700	2.53	1	–
600	1.67	1	1.30
550	1.23 } mean	1	1.34 } mean
550	1.02 } 1.08	1	1.11 } 1.17
550	0.98 }	1	1.06 }
500	0.97	1	–

4. Conclusion

Vaporization from sintered bodies and (1 0 0) and (1 1 1) surfaces of single crystals took place at a constant rate (congruent vaporization) at 500–700 °C in an air flow of $\sim$ 1 cm s^{-1} (at 20 °C). However, induction periods with smaller vaporization rates existed in the temperature range 500–600 °C, until a suitable structure for congruent vaporization was formed. From the log vaporization rates versus $1/T$ plots, activation energies were calculated to be 218 kJ mol^{-1} (sintered body) and 214 kJ mol^{-1} (1 1 1) and 201 kJ mol^{-1} (1 0 0) of the single crystal. These values are slightly smaller than the heat of vaporization (229 kJ mol^{-1}). The surface structure changed, exhibiting roofs, triangular pyramid or hexagonal faces as the vaporization proceeded. But the indices of the original faces did not change, as confirmed by XRD. The vaporization rates were discussed relating to the structure changes during heating.

Acknowledgement

The author thanks Mr Kenzi Ryu for his help with the vaporization measurements.

References

1. M. W. CHASE JR, C. A. DAVIES, J. R. DOWNEY, Jr., D. J. FRVRIP, R. A. McDONALD and A. N. SYVERUD, in "JANAF Thermochemical Tables", *J. Phys. Chem. Ref. Data* **14** (1985) Suppl. no. 1 770.
2. M. BLANDER, in "Alkalihalide Vapors" edited by P. Davidovits and D. L. McFadden, (Academic Press, New York, 1979) pp. 3–7.
3. M. ITO, T. SASAMOTO and T. SATA, *Bull. Chem. Soc. Jpn* **54** (1981) 3391.
4. T. SASAMOTO, M. ITO and T. SATA, *ibid.* **55** (1982) 3643.
5. *Idem, ibid.* **56** (1983) 2415.
6. J. HLAVAC, M. KARASEK and L. RYBARIKOWA, *Silikaty* **27** (1963) 355.
7. L. E. LEISTER and G. A. SOMORJAI, *J. Chem. Phys.* **49** (1968) 2940.
8. H. BETHGE and K. W. KELLER, *J. Cryst. Growth* **23** (1974) 105.
9. H. HOCH and H. BETHGE, *ibid.* **42** (1977) 110.
10. D. KNOPPIK and F. P. PENNINGSFELD, *ibid.* **37** (1977) 69.
11. Z. A. MUNIR, *J. Mater. Sci.* **22** (1987) 2221.
12. T. SATA and K. SAKAI, "Sintering '87", Vol. 1, edited by S. Somiya, M. Shimada, M. Yoshimura and R. Watanabe (Elsevier Applied Science, London, 1988) pp. 249–54.
13. J. C. HEYRAND and J. J. METOIS, *J. Cryst. Growth* **84** (1987) 503.

Received 29 January
and accepted 7 June 1991